J|A|C|S COMMUNICATIONS

Published on Web 05/04/2009

Facile Synthesis of Pd−Cd Nanostructures with High Capacity for Hydrogen Storage

Brian D. Adams, Guosheng Wu, Samantha Nigro, and Aicheng Chen*

Department of Chemistry, Lakehead University, Thunder Bay, Ontario P7B 5E1, Canada

Received March 8, 2009; E-mail: aicheng.chen@lakeheadu.ca

The shape-controlled synthesis of metal nanostructures has attracted considerable interest because their properties and applications are influenced greatly by their morphologies. A variety of fabrication methods have been used to produce nanostructures with different shapes.[1] Palladium is a metal which can absorb a large quantity of hydrogen and has been studied extensively in the past for this attractive property both in the gas phase[2] and under electrochemical conditions[3] because it allows a simplistic model in comparison to those of complex alloys.[4] Pd-based alloys offer a class of attractive materials for studying metal hydrides because of the higher solubility and permeability of hydrogen than pure Pd.[5] Hydrogen absorbing materials are important in hydrogen storage, metal-hydride batteries, and hydrogen purification. Herein, we report on the synthesis of novel Pd−Cd nanostructures with a high capacity for hydrogen storage. To the best of our knowledge, there is no report on or study of Pd−Cd nanostructured materials in the literature. The cheap cost of Cd makes it an attractive material to combine with Pd, and our study shows that the addition of Cd significantly enhances the hydrogen sorption capacity of Pd.

In this study, a series of Pd−Cd nanostructures with compositions of Cd ranging from 0 at% to 20 at% were directly grown onto Ti substrates using a facile hydrothermal reduction method. The amount of Pd in the coatings was kept constant while various amounts of Cd were added. The average atomic compositions of the formed nanostructures were determined with the use of an energy dispersive X-ray spectrophotometer (EDS); they were consistent with the ratio of Pd and Cd precursors initially added to the hydrothermal vessels. This is further confirmed by our ICP analysis as shown in the Supporting Information (Table S1).

Typical SEM images of the formed Pd−Cd nanostructures are displayed in Figure 1, showing that the addition of Cd drastically changes the morphology. Pure Pd (Figure 1a) exhibits nanoporous morphology with randomized small particles. The addition of small amounts of Cd (as little as 1.5%) triggers the formation of dendrites. The formed dendrites decrease in size with increasing amounts of Cd from 1.5% (Figure 1b) to 15.0% (Figure 1e). The morphology of the Pd−Cd materials with 10% Cd tends to be very similar to that of those with a composition of 15%. Further increasing the Cd content to 20%, a porous Pd−Cd thin film is formed, mainly consisting of large particles ranging in size from 50 nm to 1 μm (Figure 1f).

X-ray diffraction (XRD) was used to identify the internal crystalline structures of the prepared Pd−Cd nanomaterials. As seen in Figure 2, the XRD patterns show that all of the peaks, except those arising from the Ti substrates, can be referenced to a face-centered cubic (fcc) unit cell. For pure Pd, the 2θ values of 40.02°, 46.56°, 68.04°, and 82.05° can be indexed to the diffraction of (111), (200), (220), and (311) planes of Pd, respectively (JCPDS file no. 46-1043). As more Cd is added, all the peaks are shifted slightly to smaller 2θ values, indicative of increased d-spacing and a dilation of the lattice constant, due to the incorporation of increasing amounts of the larger Cd atoms into the Pd fcc lattice. No hexagonal Cd peaks appear, indicating that alloyed Pd−Cd intermetallic nanostructures were formed. The lattice constants

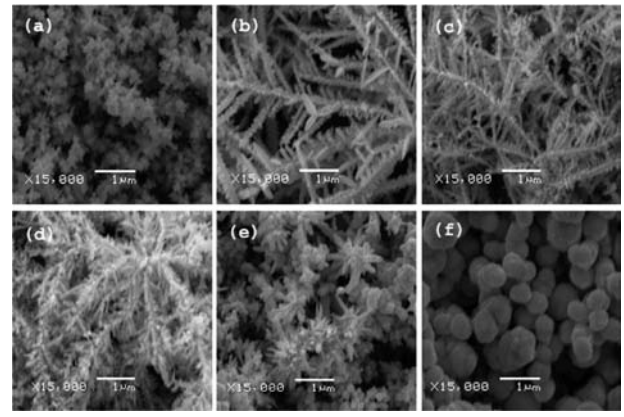

Figure 1. SEM images at 15 000× magnification of the Pd−Cd surfaces with normalized atomic ratios of Pd/Cd of 100:0 (a); 98.5:1.5 (b); 97:3 (c); 95:5 (d); 85:15 (e); and 80:20 (f).

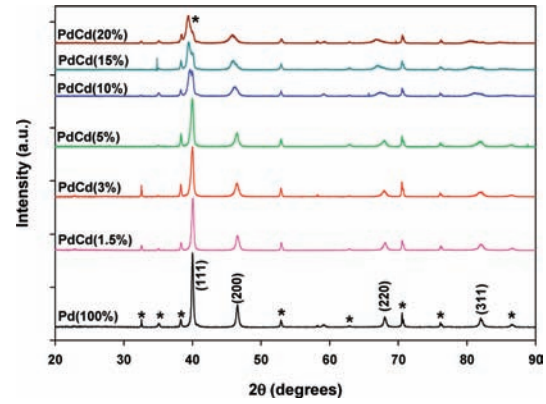

Figure 2. XRD patterns of the prepared PdCd films. Diffraction peaks belonging to the Ti substrate are labeled with (*).

were calculated from the (220) peak.[6] Pure Pd had a lattice constant of 0.389 nm while the Pd−Cd(20%) had a lattice constant of 0.396 nm. The dependence of the lattice constant on the composition obeys Vegard's law which is common for many binary intermetallic compounds (see Figure S1).

It is generally assumed that hydrogen diffuses into a perfect palladium crystal by jumping from one octaedric site to another.[3a] Due to the dilation of the lattice constant by the addition of Cd, the diffusion of hydrogen is expected to increase.[7] The capacity of the prepared Pd−Cd nanostructures for hydrogen adsorption/absorption was studied with cyclic voltammetry. Figure 3 shows cyclic voltammograms recorded in the range −200 to 400 mV at a scan rate of 20 mV/s. Under the acid conditions used here, the region of hydrogen sorption/desorption can be clearly separated from the potential of the palladium oxide formation, which is contrary to the situation in alkaline solutions;[8] however it is difficult to decouple adsorption from absorption.[3b] The total charge, Q_H, due to hydrogen adsorption and absorption in the

10.1021/ja901798u CCC: $40.75

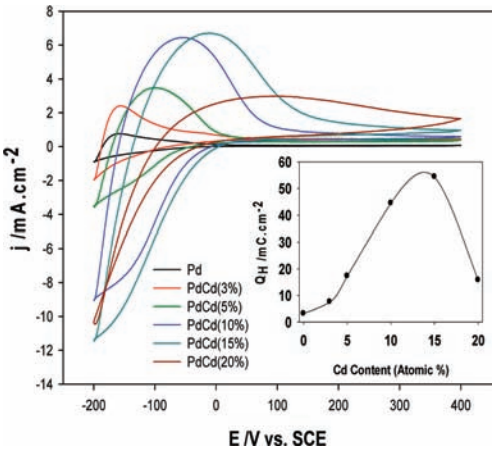

Figure 3. Cyclic voltammograms of the Pd−Cd electrodes in 0.1 M $HClO_4$ performed with a scan rate of 20 mV/s. The overall hydrogen desorption charge Q_H vs the normalized atomic composition of Cd is shown in the inset.

Pd−Cd nanostructures, was obtained by integrating the area under the anodic peaks in the cyclic voltammograms. The charges for hydrogen desorption on the Pd−Cd nanostructures with 0%, 3%, 5%, 10%, 15%, and 20% Cd were 3.20, 7.57, 17.28, 44.45, 54.38, and 15.79 mC/cm^2, respectively. The Pd−Cd nanostructures with 10−15% Cd possess the highest capacity for hydrogen adsorption/absorption, but the H/Pd ratio is much lower than the upper limit of the H/Pd ratio (∼0.7) reported in the literature.[3b,9c] This is due to the fact that our electrodes are not saturated with hydrogen in the cyclic voltammetric measurements. Increasing the Cd to 20% dramatically decreases the hydrogen adsorbing/absorbing capacity. The formation of the large Pd−Cd particles as evidenced in Figure 1f decreases the active surface area, thus lowering the hydrogen sorption capacity. It is known that properties of nanomaterials depend on the size of their crystallites.[3b,9] A small crystallite size increases the number of grain boundaries in which hydrogen can be stored.[3b,5,9a] The average crystallite size of the Pd−Cd nanostructured alloys was calculated from the (200) peak (Figure 2) using the Scherrer equation.[10] As seen in Figure S2, the average size of the crystallite decreased as the amount of Cd was increased. When the amount of Cd was increased from 0% to 15%, the crystallite size decreased from 25.81 to 9.16 nm and their BET surface area was increased from 11.58 to 46.64 m^2/g, thus greatly enhancing the capacity for hydrogen sorption.

Based on computational modeling,[11] it is believed that dendritic growth reflects a competition between order associated with the symmetries of the crystal structure and morphological instabilities arising from the nonlinear diffusion process.[11d] Simulations of the morphology of a diffusion-limited aggregate show that a change in the random noise level can vary the morphology from an ordered anisotropic shape into an irregular branching pattern.[11a] In the present work, 100% Pd species, when reduced, did not produce dendritic morphology, while the presence of small amounts of Cd massively triggers dendritic growth. The Cd atoms at low percentages (e.g., 1.5%, 3%, and 5%) can be treated as "foreign impurities" with respect to the Pd matrix. This could correspond to the aforementioned "instabilities" in crystal growth and "random noise" in computer simulations, both of which are essential for inducing dendritic growth. In the case of our hydrothermal process, the reducing agent ammonium formate is always present in large excess compared to the metal precursors. This ensures the coreduction of both metal cations and produces sufficiently fast reaction kinetics to cause supersaturation during the crystal nucleation phase. In the subsequent crystal growth phase, diffusion of the reduced Pd and Cd is the dominant driving force responsible for the dendritic growth. When a small amount of Cd is introduced, the reduced Cd species serve as "pinning centers" and interfere with the growth front of the main trunks. Since the interfering Cd atoms have the possibility of occupying certain crystal lattice points during the diffusion process, and the anisotropic growth of Pd atoms along the preferred crystal lattice is kinetically fast enough to engulf the Cd atoms and further accommodate these foreign atoms inside the crystal lattice, the formed intermetallic nanocrystals are consistent in composition with the original aqueous mixture of the precursors. This is further supported by our EDS analysis and ICP results (Table S1).

In conclusion, we synthesized and studied, for the first time, Pd−Cd nanostructures with controllable and reproducible compositions. Our study demonstrates that the addition of Cd significantly changes the morphology and properties of the formed Pd−Cd nanostructures. Our electrochemical measurements show that the Pd−Cd nanostructures with 10−15% of Cd possess the highest capacity for hydrogen sorption, over 15 times greater than the nanoporous Pd networks (Figure 1a). The significant enhancement by Cd can be attributed to a combination of the formation of small dendritic structures, dilation of the lattice constant, and decrease of the crystallite size. The facile approach reported in this communication opens a door to develop high performance Pd−Cd nanomaterials for hydrogen storage.

Acknowledgment. This work was supported by a Discovery Grant from the Natural Sciences and Engineering Research Council of Canada (NSERC). A.C. acknowledges NSERC and the Canada Foundation of Innovation (CFI) for the Canada Research Chair Award in Material and Environmental Chemistry.

Supporting Information Available: Experimental details, ICP results, Vegard's plot, and the Pd−Cd particle size. This material is available free of charge via the Internet at http://pubs.acs.org.

References

(1) (a) Wang, J.; Thomas, D. F.; Chen, A. *Chem. Commun.* **2008**, 5010–5012. (b) Zhang, Y.-J.; Zhang, Y.; Wang, Z.-H.; Li, D.; Cui, T.-Y.; Zhang, Z.-D. *Eur. J. Inorg. Chem.* **2008**, 2733–2738. (c) Wang, H.; Brandl, D. W.; Le, F.; Nordlander, P.; Halas, N. J. *Nano Lett.* **2006**, *6*, 827–832.

(2) (a) Kishore, S.; Nelson, J. A.; Adair, J. H.; Eklund, P. C. *J. Alloy Compd.* **2005**, *389*, 234–242. (b) Yamauchi, M.; Ikeda, R.; Kitagawa, H.; Takata, M. *J. Phys. Chem. C* **2008**, *112*, 3294–3299. (c) Kobayashi, H.; Yamauchi, M.; Kitagawa, H.; Kubota, Y.; Kato, K.; Takata, M. *J. Am. Chem. Soc.* **2008**, *130*, 1828–1829.

(3) (a) Gabrielli, C.; Grand, P. P.; Lasia, A.; Perrot, H. *J. Electrochem. Soc.* **2004**, *151*, A1925−A1936. (b) Gabrielli, C.; Grand, P. P.; Lasia, A.; Perrot, H. *J. Electrochem. Soc.* **2004**, *151*, A1937−A1942. (c) Losiewicz, B.; Birry, L.; Lasia, A. *J. Electroanal. Chem.* **2007**, *611*, 26–34. (d) Duncan, H.; Lasia, A. *Electrochim. Acta* **2008**, *53*, 6845–6850.

(4) (a) Chen, Y.; Sequeira, C.; Allen, T.; Chen, C. P. *J. Alloy Compd.* **2005**, *404−406*, 661–664. (b) Jeng, R.-R.; Lee, S.-L.; Hsu, C.-W.; Wu, Y.-P.; Lin, J.-C. *J. Alloy Compd.* **2008**, *464*, 467–471. (c) Visintin, A.; Tori, L. A.; Gaaventta, G.; Triaca, W. E. *J. Electrochem. Soc.* **1998**, *145*, 4169–4172.

(5) Sun, Y.; Tao, Z.; Chen, J.; Herricks, T.; Xia, Y. *J. Am. Chem. Soc.* **2004**, *126*, 5940–5941.

(6) Huang, Y.; Zhou, X.; Liao, J.; Liu, C.; Lu, T.; Xing, W. *Electrochem. Commun.* **2008**, *10*, 1155–1157.

(7) Barlag, H.; Opara, L.; Zuchner, H. *J. Alloy Compd.* **2002**, *330−332*, 434–437.

(8) (a) Czerwinski, A.; Kiersztyn, I.; Grden, M.; Czapla, J. *J. Electroanal. Chem.* **1999**, *471*, 190–195. (b) Bolzan, A. E. *J. Electroanal. Chem.* **1995**, *380*, 127–138. (c) Yang, L.; Cheng, Y.-T. *Int. J. Hydrogen Energy* **1996**, *21*, 281–291.

(9) (a) Stur, H.; Striffler, T.; Wipf, H.; Natter, H.; Wettmann, B.; Janssen, S.; Hemplemann, R.; Hahn, H. *J. Alloy Compd.* **1997**, *253−254*, 393–396. (b) Fagherazzi, G.; Canton, P.; Riello, P.; Pernicone, N.; Pinna, F.; Battagliarin, M. *Langmuir* **2000**, *16*, 4539–4536. (c) Amorin, C.; Keane, M.-A. *J. Colloid Interface Sci.* **2008**, *322*, 196–208.

(10) Baranova, E. A.; Le Page, Y.; Ilin, D.; Bock, C.; MacDougall, B.; Mercier, P. H. *J. Alloy Compd* **2009**, *471*, 387–394.

(11) (a) Ben-Jacob, E.; Garik, P. *Nature* **1990**, *343*, 523–530. (b) Gránásy, L.; Pusztai, T.; Warren, J. A.; Douglas, J. F.; Borzsonyi, T.; Ferreiro, V. *Nat. Mater.* **2003**, *2*, 92–96. (c) Haxhimali, T.; Karma, A.; Gonzales, F.; Rappaz, M. *Nat. Mater.* **2006**, *5*, 660–664. (d) Imai, H. *Top. Curr. Chem.* **2007**, *270*, 43–72. (e) Fleury, V. *Nature* **1997**, *390*, 145–148.

JA901798U